



# CHORUS

This is the accepted manuscript made available via CHORUS. The article has been published as:

## $^{239}\text{Pu}$ nuclear magnetic resonance in the candidate topological insulator $\text{PuB}_4$

A. P. Dioguardi, H. Yasuoka, S. M. Thomas, H. Sakai, S. K. Cary, S. A. Kozimor, T. E. Albrecht-Schmitt, H. C. Choi, J.-X. Zhu, J. D. Thompson, E. D. Bauer, and F. Ronning

Phys. Rev. B **99**, 035104 — Published 2 January 2019

DOI: [10.1103/PhysRevB.99.035104](https://doi.org/10.1103/PhysRevB.99.035104)

# $^{239}\text{Pu}$ nuclear magnetic resonance in the candidate topological insulator $\text{PuB}_4$

A. P. Dioguardi,<sup>1,2,\*</sup> H. Yasuoka,<sup>1,3</sup> S. M. Thomas,<sup>1</sup> H. Sakai,<sup>4,1</sup> S. K. Cary,<sup>1</sup> S. A. Kozimor,<sup>1</sup> T. E. Albrecht-Schmitt,<sup>5</sup> H. C. Choi,<sup>1</sup> J.-X. Zhu,<sup>1</sup> J. D. Thompson,<sup>1</sup> E. D. Bauer,<sup>1</sup> and F. Ronning<sup>1</sup>

<sup>1</sup>*Los Alamos National Laboratory, Los Alamos, New Mexico 87545, USA*

<sup>2</sup>*IFW Dresden, Institute for Solid State Research, P.O. Box 270116, D-01171 Dresden, Germany*

<sup>3</sup>*Max Planck Institute for Chemical Physics of Solids, 01187 Dresden, Germany*

<sup>4</sup>*Advanced Science Research Center, Japan Atomic Energy Agency, Tokai, Naka, Ibaraki 319-1195, Japan*

<sup>5</sup>*Department of Chemistry and Biochemistry, Florida State University, 95 Chieftan Way, Tallahassee, Florida 32306*

(Dated: December 17, 2018)

We present a detailed nuclear magnetic resonance (NMR) study of  $^{239}\text{Pu}$  in bulk and powdered single-crystal plutonium tetraboride ( $\text{PuB}_4$ ), which has recently been investigated as a potential correlated topological insulator. This study constitutes the second-ever observation of the  $^{239}\text{Pu}$  NMR signal, and provides unique on-site sensitivity to the rich  $f$ -electron physics and insight into the bulk gap-like behavior in  $\text{PuB}_4$ . The  $^{239}\text{Pu}$  NMR spectra are consistent with axial symmetry of the shift tensor showing for the first time that  $^{239}\text{Pu}$  NMR can be observed in an anisotropic environment and up to room temperature. The temperature dependence of the  $^{239}\text{Pu}$  shift, combined with a relatively long spin-lattice relaxation time ( $T_1$ ), indicate that  $\text{PuB}_4$  adopts a non-magnetic state with gap-like behavior consistent with our density functional theory (DFT) calculations. The temperature dependencies of the NMR Knight shift and  $T_1^{-1}$ —microscopic quantities sensitive only to bulk states—imply bulk gap-like behavior confirming that  $\text{PuB}_4$  is a good candidate topological insulator. The large contrast between the  $^{239}\text{Pu}$  orbital shifts in the ionic insulator  $\text{PuO}_2$  ( $\sim +24.7\%$ ) and  $\text{PuB}_4$  ( $\sim -0.5\%$ ) provides a new tool to investigate the nature of chemical bonding in plutonium materials.

PACS numbers: 76.60.-k, 76.60.Es

Topological insulators have received much attention recently due to the experimental verification of the theoretical prediction of topologically nontrivial symmetry-protected surface states [1, 2]. Kondo insulators are  $f$ -electron systems with strong correlations in which hybridization of the  $f$ -electrons with conduction electrons forms a gap at the Fermi level [3]. Strong spin-orbit coupling can result in a topological Kondo insulator in which band inversion drives the emergence of nontrivial topologically protected gapless surface states [4, 5]. Samarium hexaboride ( $\text{SmB}_6$ ) is the primary candidate example of a topological Kondo insulator [6–9]. As compared with rare-earth  $4f$ -electron systems, the actinide  $5f$ -electron systems have more spatially-extended  $f$ -electron wave functions, which generally results in an enhancement of the energy scales involved [10–12]. Plutonium (Pu) materials display particularly complex physical properties due to the  $5f$ -electrons lying on the brink between bonding and non-bonding configurations [13, 14]. For example, elemental Pu forms in six allotropes at ambient pressure that vary in density by up to 25% [15, 16]. Pu compounds display a wide variety of electronic ground states including heavy-fermion behavior, magnetism, superconductivity [17], and most recently the prediction of topologically non-trivial states [12, 18].

Very recently, plutonium tetraboride ( $\text{PuB}_4$ ) has been theoretically predicted to be a strong topological insulator in which electronic correlations play an important role [19]. The density functional theory (DFT) calculations predict a band gap  $\Delta \sim 254$  meV and dynamical mean-field theory (DMFT) calculations find that elec-

tronic correlations significantly reduce the magnitude of the predicted energy gap. Experimental measurements from the same work find an increase of the resistivity with decreasing temperature and saturation at low temperature reminiscent of the behavior of  $\text{SmB}_6$  [20]. Fits to the temperature dependent resistivity yield an energy gap  $\Delta = 35$  meV, which is taken as evidence for correlation-induced suppression of the expected gap value.  $\text{PuB}_4$  forms in the tetragonal  $\text{ThB}_4$ -type crystal structure with space group  $P4/mbm$  (# 127) as shown in Fig. 1(a) and was first reported nearly 60 years ago [21–23]. Magnetic measurements of  $\text{PuB}_4$  indicated that the Pu magnetic moment is very small, on the order of  $7.2 \times 10^{-4}$  emu/mol and shows little temperature dependence [24]. This small magnetic susceptibility and insulating-like electrical transport make  $\text{PuB}_4$  an ideal material in which to search for  $^{239}\text{Pu}$  nuclear magnetic resonance (NMR).

NMR is a powerful tool for the investigation of the physics and chemistry of condensed matter in general [27–30]. The  $^{239}\text{Pu}$  nucleus has nuclear spin  $I = \frac{1}{2}$  and is of great interest as an on-site probe of the rich  $f$ -electron physics of Pu. The first attempt to observe  $^{239}\text{Pu}$  NMR was performed on  $\alpha$ -Pu more than 50 years ago [31], however to date there is only a single report of  $^{239}\text{Pu}$  NMR [26] in the ionic insulator  $\text{PuO}_2$ . The main difficulty involved in observing  $^{239}\text{Pu}$  NMR—and other  $f$ -electron nuclei, in general—can be traced to the very strong hyperfine fields at the nucleus produced by on-site hyperfine coupling to the  $f$ -electrons. Consequently, the resulting spectral width can be very large, and the

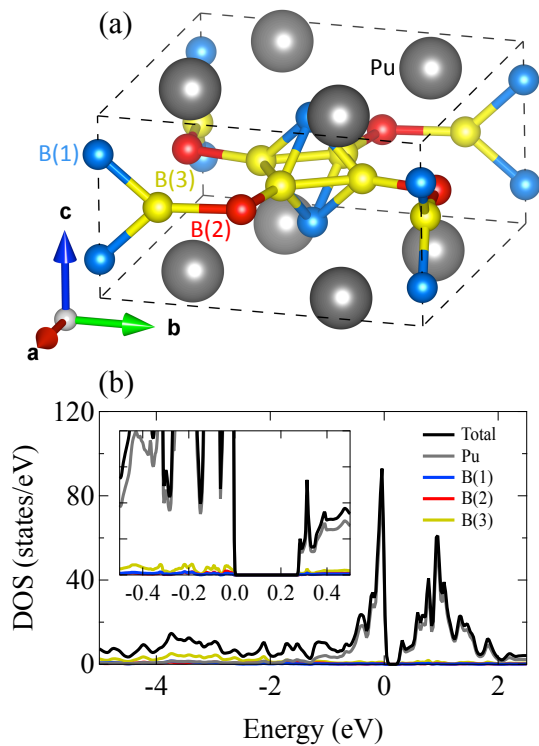


FIG. 1. (a) Unit cell of  $\text{PuB}_4$  illustrating the single plutonium site and three inequivalent boron sites [25]. (b) Density of states (DOS) and partial DOS as a function of energy calculated within density functional theory including spin-orbit coupling. The inset shows an expanded region near the Fermi energy where there is an energy gap of  $\Delta \sim 254$  meV.

spin-lattice ( $T_1$ ) and spin-spin ( $T_2$ ) relaxation times can be extremely short, which makes detection of the signal difficult. These effects can be minimized in systems with a gap in the electronic and spin excitation spectrum, as evident in the case of  $\text{PuO}_2$ ,  $\text{UO}_2$ , and  $\text{YbB}_{12}$  [26, 32, 33].

Here we report the observation of, and the microscopic properties extracted from  $^{239}\text{Pu}$  NMR in powdered and single crystalline  $\text{PuB}_4$ . Crystals were grown by an Al-flux method and sample preparation details are provided in the Supplementary Material [34]. We deduce the resonant condition of  $^{239}\text{Pu}$  in  $\text{PuB}_4$   $^{239}\gamma(1 + K_{\text{PuB}_4})/2\pi = 2.288 \pm 0.001$  MHz/T from the powder spectra, and find axial symmetry of the hyperfine interaction on the Pu site. Both the powder and the single crystal Knight shift  $K(T)$  of  $^{239}\text{Pu}$  show temperature dependence consistent with gap-like behavior with a static energy gap (extracted from the single crystalline  $K_c(T)$  data)  $\Delta_K \approx 156$  meV. The relaxation time is quite long—on the order of milliseconds to seconds—even at the  $^{239}\text{Pu}$  site, indicating that the  $f$ -electron configuration is non-magnetic. The dominant temperature dependence of the spin-lattice relaxation rate  $T_1^{-1}(T)$  also shows gap-like behavior with a dominant dynamic gap  $\Delta_{T_1} \approx 251$  meV. We compare our experimental NMR results with the density of states, cal-

culated within density functional theory including spin-orbit coupling, which finds a gap of similar order of magnitude. A weak low-temperature peak in  $T_1^{-1}(T)$  indicates the presence of bulk in-gap magnetic states with a gap  $\delta \approx 2$  meV.

Our DFT calculations including spin-orbit coupling reveal a gap in the density of states (DOS) at the Fermi energy  $E_F$  of roughly 254 meV as shown in Fig. 1(b). To account for the presence of correlations we also performed DFT + DMFT calculations. Using a  $U$  of 4.5 eV and high-order Slater integrals amounting to an effective  $J = 0.512$  eV [35, 36] and attempting to stabilize a magnetic solution, we find that the self-consistent solution recovers a non-magnetic state with a band gap at the Fermi level of order 10.3 meV (see Supplemental Material for further calculation details [34]). The appreciable calculated gap in the DOS combined with an expected non-magnetic ground state indicate the probable absence of strong spin- and charge-relaxation channels, and therefore, we expect the spin-lattice relaxation rate in  $\text{PuB}_4$  to be long enough to observe the  $^{239}\text{Pu}$  signal. The  $^{239}\text{Pu}$  nucleus has  $I = \frac{1}{2}$  and the bare gyromagnetic ratio was determined based on the initial observation in  $\text{PuO}_2$  to be  $^{239}\gamma/2\pi = 2.29 \pm 0.001$  MHz/T [26]. Consequently, we would expect to find an NMR signal in the field range of roughly 7 to 9 T with an rf excitation frequency  $f_0 \sim 20$  MHz. Indeed, for  $f_0 = 20.222$  MHz we discovered an asymmetric powder spectrum between 8.80 and 8.92 T as shown in Fig. 2(a-b). To establish that the observed signal is indeed due to  $^{239}\text{Pu}$  from  $\text{PuB}_4$  field-swept spectra were collected at several frequencies. These spectra are shown in Fig. 2(a) and they confirm the intrinsic nature of the NMR signal.

The crystal structure of  $\text{PuB}_4$  has a single Pu site with oriented site symmetry  $m.2m$  (see Fig. 1(a)). For each crystallite in the powdered sample the resonance condition can be expressed as  $2\pi f_0 = \gamma B_0(1 + K_i)$  where  $K_i$  are the elements of the shift tensor for a given field orientation and  $B_0$  is the magnetic field at which the resonance occurs for frequency  $f_0$ . Although the local symmetry is orthorhombic in principle, the non-axial components of the shift tensor are found to be extremely close to zero from the spectral pattern in Fig. 2(b), *i.e.*, it can be practically regarded to be tetragonal. Assuming tetragonal symmetry for the hyperfine interaction on Pu, the isotropic and axial shifts ( $K_{iso}$  and  $K_{ax}$ , respectively) are extracted from the observed  $K_c$  and  $K_{ab}$  using  $K_{iso} = (K_c + 2K_{ab})/3$  and  $K_{ax} = (K_c - K_{ab})/3$ , where the angular dependence of the shift is given by  $K(\theta) = K_{iso} + K_{ax}(3 \cos^2 \theta - 1)$ .

The isotropic shift of  $^{239}\text{Pu}$  in  $\text{PuB}_4$  is  $K_{iso}(T = 4 \text{ K}) = -0.09 \pm 0.04$  % is obtained from the slope in the frequency vs. field plot in Fig. 2(a). This value is notably different from the shift  $K(T = 4 \text{ K}) = 24.72 \pm 0.04$  % of  $^{239}\text{Pu}$  in  $\text{PuO}_2$  [26]. To calculate these shifts we have assumed the bare  $^{239}\gamma/2\pi = 2.29$  MHz/T as de-

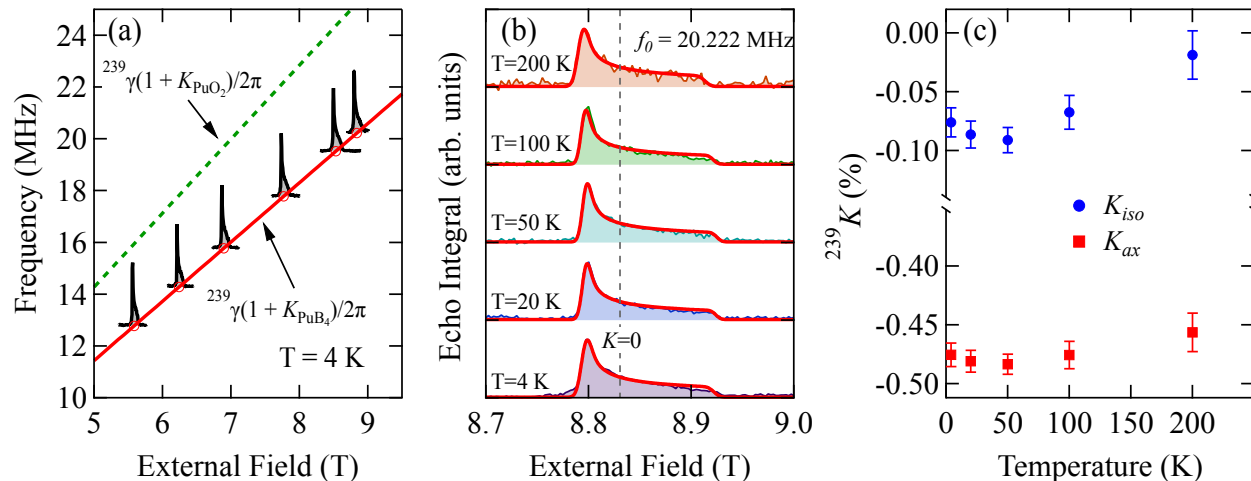


FIG. 2. (a)  $^{239}\text{Pu}$  nuclear magnetic resonance (NMR) field-swept spectra of powdered single crystals of  $\text{PuB}_4$  at several frequencies at  $T = 4$  K. Spectra are normalized to the maximum value and offset vertically so as to correspond to the observed frequency  $f_0$  on the left axis. Red circles and line indicate the resonant condition of  $^{239}\text{Pu}$  in  $\text{PuB}_4$   $^{239}\gamma(1 + K_{\text{PuB}_4})/2\pi = 2.288 \pm 0.001$  MHz/T (at  $T = 4$  K) and green dashed line shows  $^{239}\gamma(1 + K_{\text{PuO}_2})/2\pi = 2.856 \pm 0.001$  MHz/T as determined previously [26]. (b)  $^{239}\text{Pu}$  NMR field-swept spectra at  $f_0 = 20.222$  MHz offset vertically for several temperatures. Solid red curves are best fits as described in the text. Vertical dashed line indicates zero shift  $K = 0$  using  $^{239}\gamma/2\pi = 2.29$  MHz/T. (c)  $^{239}K_{iso}$  and  $^{239}K_{ax}$  vs temperature extracted from fits in (b).

terminated from the study of  $\text{PuO}_2$  [26].  $K_{ax}(T = 4 \text{ K}) = -0.48 \pm 0.01$  % is also significantly different from the shift found in  $\text{PuO}_2$  [26] at the same temperature. It is worth noting that the relatively small absolute value of  $K_{ax}$  was crucial to find the  $^{239}\text{Pu}$  signal in an anisotropic environment.

The temperature dependence of the field-swept spectra at  $f_0 = 20.222$  MHz and the corresponding least-squares fits are shown in Fig. 2(b). An axially symmetric shift tensor remains a good approximation for all temperatures measured. Fig. 2(c) illustrates that  $K_{iso}$  has a small negative value with a positive temperature dependence, and  $K_{ax}$  has a larger negative value with a smaller temperature dependence relative to  $K_{iso}$ . In general,  $K_{iso}$  originates from the spin-polarized Fermi contact interaction and couples to the uniform spin susceptibility via the hyperfine interaction.  $K_{ax}$  may be dominantly attributed to the temperature independent orbital hyperfine interaction with a small temperature dependence resulting from a reduction of the anisotropy of the spin susceptibility with increasing temperature. The facts that the spin-lattice relaxation time in  $\text{PuB}_4$  is sufficiently long to enable the observation of  $^{239}\text{Pu}$  NMR, and that Knight shifts are weakly temperature dependent imply that the electronic state of Pu in  $\text{PuB}_4$  is nearly nonmagnetic. Assuming a local picture this implies either that Pu has a  $5f^6$  configuration or  $\text{PuB}_4$  adopts a Kondo insulating state.

Finally, we performed measurements on a single crystal of  $\text{PuB}_4$  for the external field applied along the  $\hat{c}$ -axis. We

measured both the  $\hat{c}$ -axis  $^{239}\text{Pu}$  shift  $K_c$  and  $T_1^{-1}$  as a function of temperature up to 300 K as shown in Fig. 3. We fit the  $^{239}\text{Pu}$  inversion recovery curves to the form

$$M_N(t) = M_N(\infty) \left( 1 - \alpha e^{-(t/T_1)^\beta} \right), \quad (1)$$

where  $M_N(\infty)$  is the equilibrium nuclear magnetization,  $\alpha$  is the inversion fraction,  $T_1$  is the spin-lattice relaxation time, and  $\beta$  is a stretching exponent that modifies the expected single exponential behavior ( $\beta = 1$ ). We find that  $\beta_{avg} = 0.813$ , which is a measure of the width of the probability distribution of  $T_1$  [37], is independent of temperature and may indicate sensitivity to self-irradiation induced disorder [38]. Both  $K_c$  and  $T_1^{-1}$  are consistent with gap-like behavior, and  $T_1^{-1}$  exhibits a low temperature maximum consistent with the presence of in-gap states which are suppressed with applied magnetic field as shown in the inset of Fig. 3.

From a chemistry perspective, the  $^{239}\text{Pu}$  orbital shift is very different between  $\text{PuO}_2$  ( $\sim +24.7$  % [26]) and  $\text{PuB}_4$  ( $\sim -0.5$  %). The origin of the difference in magnitude of the orbital shift is clear from the fact that in the case of  $\text{PuO}_2$  the Pu ion has a completely ionic  $\text{Pu}^{4+}$  ( $5f^4$ ) state and experiences strong cubic crystalline electronic field giving rise to a non-magnetic ground state with a Van Vleck orbital magnetism, which is the main source of the hyperfine interaction to the Pu nuclear moment. In contrast, DFT + DMFT calculations point to  $\text{PuB}_4$  being a strongly correlated insulator with possible strong topological character, similar to the case of  $\text{SmB}_6$ . In  $\text{SmB}_6$

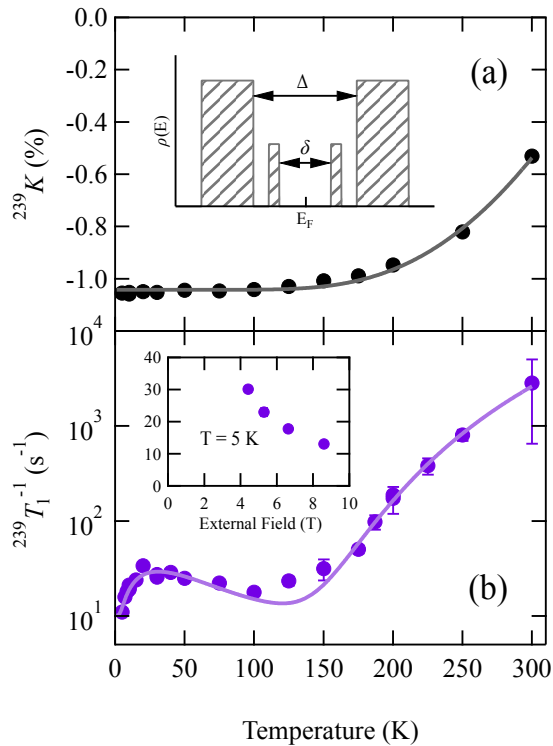


FIG. 3. Single crystal  $^{239}\text{Pu}$  NMR data for external field aligned along the crystalline  $\hat{c}$  direction. (a) Shift  $K_c$  vs. temperature and fit (solid line) to gap-like behavior as discussed in the text which yields an energy gap  $\Delta_K = 155.6 \pm 11.0$  meV, but is not sensitive to the in-gap states. The inset shows the model density of states  $\rho(E)$  vs. energy  $E$  employed in the fits. (b) Spin-lattice relaxation rate  $T_1^{-1}$  vs. temperature and fit (solid line) to gap-like behavior as discussed in the text which yields energy gaps  $\Delta_{T_1} = 251.3 \pm 49.4$  meV and  $\delta = 1.8 \pm 2.4$  meV. The external field was adjusted (from 8.5900 T at 5 K to 8.5455 T at 300 K) such that the observed frequency was  $f_0 = 19.465$  MHz for all temperatures. The inset shows the field dependence of  $T_1^{-1}$  at  $T = 5$  K indicating the suppression of in-gap states with applied external field.

the gap arises from hybridization between  $4f$  and ligand electrons that give rise to a pronounced non-integral value of the  $4f$  configuration. Our results suggest that this is also the case in  $\text{PuB}_4$ . The large difference in orbital shift between  $\text{PuO}_2$  and  $\text{PuB}_4$  clearly indicates that  $^{239}\text{Pu}$  NMR is highly sensitive to the degree of bond mixing and the  $f$ -electron configuration. Furthermore, the relaxation time is roughly two orders of magnitude shorter than in  $\text{PuO}_2$  [26], which likely reflects the difference in chemical environments between  $\text{PuB}_4$  and  $\text{PuO}_2$ .

The capability to measure  $^{239}\text{Pu}$  was key to observing gap-like behavior in the static and dynamic spin-susceptibilities as evidenced by the temperature dependencies of  $K_c$  and  $T_1^{-1}$  shown in Fig. 3. Our  $^{11}\text{B}$  measurements of the temperature dependence of the Knight shift (see Supplemental Material [34]) do not show any evi-

dence of gap-like behavior, likely due to the much smaller value of the hyperfine coupling of the  $^{11}\text{B}$  nuclei to the electrons as compared to the  $^{239}\text{Pu}$  hyperfine coupling, which is expected to be on the order of  $150 \text{ T}/\mu_B$ . Therefore, our  $^{239}\text{Pu}$  NMR results are sensitive to otherwise enigmatic physics in  $\text{PuB}_4$ .

There exist a number of previous NMR studies that find gap-like behavior of  $f$ -electron systems, *e.g.*  $\text{SmB}_6$  [39, 40],  $\text{YbB}_{12}$  [33],  $\text{Ce}_3\text{Bi}_4\text{Pt}_3$  [41]. Here we follow the analysis scheme of  $\text{SmB}_6$  [40] by fitting the temperature dependence of the  $^{239}\text{Pu}$  Knight shift and spin-lattice relaxation rate by assuming a simple model for the density of states near the Fermi energy. The Knight shift is given by,

$$K(T) \propto \int f(E, T)[1 - f(E, T)]\rho(E)dE, \quad (2)$$

where  $f(E, T)$  is the Fermi function and  $\rho(E)$  is the density of states. The spin-lattice relaxation rate is given by,

$$T_1^{-1}(T) \propto \int f(E, T)[1 - f(E, T)]\rho(E)^2 dE. \quad (3)$$

We assume a simplified model of the density of states (equivalent to that of Caldwell *et al.* [40]) given by,

$$\begin{aligned} \rho(E) &= \rho_i(T) \text{ for } \delta < |E| < W_i \\ &= \rho \text{ for } \Delta < |E| < W, \end{aligned} \quad (4)$$

and zero otherwise as shown in the inset of Fig. 3(a). We perform least-squares fits using a Levenberg-Marquardt minimization algorithm which iteratively recalculates the model function via numerical integration of Eqns. 2 and 3 (see Supplemental Material for a full description of the curve fitting [34]). The energy gap extracted from the Knight shift  $\Delta_K = 155.6 \pm 11.0$ . For the Knight shift we find no indication of the presence of in-gap states, that is  $\rho_i(T) = 0$ , similar to the static susceptibility of  $\text{SmB}_6$  [40]. The dominant energy gap extracted from the spin-lattice relaxation  $\Delta_{T_1} = 251.3 \pm 49.4$  meV. A smaller in-gap density of states  $\rho_i(T) = \rho_{i0}e^{-T/T_0}$  with an energy gap  $\delta = 1.8 \pm 2.4$  meV was also found to be consistent with the small low temperature enhancement of  $T_1^{-1}(T)$ . The discrepancy between the static gap  $\Delta_K$  and the dynamic gap  $\Delta_{T_1}$  has been observed in numerous spin-gap systems [42] and is related to differences in the processes that contribute to the Knight shift and the spin-lattice relaxation. In the majority of these spin-gap systems the dynamic gap  $\Delta_{T_1} > \Delta_K$  and on average  $\Delta_{T_1}/\Delta_K = 1.73$ . In the case of  $\text{PuB}_4$  we find  $\Delta_{T_1}/\Delta_K = 1.6 \pm 0.3$ .

While NMR is not sensitive to the surface states in bulk powders or single crystals [43], it is a powerful microscopic probe of the bulk properties of topological materials. Our  $^{239}\text{Pu}$  NMR results are consistent with a bulk gap which is only slightly suppressed from the DFT+SOC calculated value of 254 meV. In addition to

the dominant gap-like behavior evidenced by  $K_c(T)$  and  $T_1^{-1}(T)$ , we also find a small peak at low temperature that is reminiscent of the  $^{11}\text{B}$   $T_1^{-1}(T)$  in  $\text{SmB}_6$  [39] and  $\text{YbB}_{12}$  [33]. In  $\text{SmB}_6$  the peak is thought to be due to bulk magnetic in-gap states, and while the nature of these states is still controversial, it has been suggested that these states are identical to the topologically protected surface states [44]. In  $\text{PuB}_4$  we find that  $T_1^{-1}(T = 5 \text{ K})$  is strongly field dependent as shown in the inset of Fig. 3(b), which is similar to previous field dependent measurements of  $\text{SmB}_6$  [40].

These results motivate further investigation of the field and Pu-substitution dependence of  $T_1^{-1}$  over a wide temperature range. Previous transport measurements find a much smaller gap  $\Delta = 35 \text{ meV}$  [19]. This is also the case in  $\text{YbB}_{12}$ , where NMR finds a larger gap than resistivity, and may be related to the presence of in-gap states which account for the low temperature enhancement in  $T_1^{-1}$ . This discrepancy motivates Hall coefficient measurements in  $\text{PuB}_4$  (which in  $\text{YbB}_{12}$  agree with the NMR-measured gap), as well as surface-sensitive tunneling or spin-polarized ARPES measurements. Finally, we note that measurements comparing  $^{11}\text{B}$  and  $^{10}\text{B}$   $T_1^{-1}$  in  $\text{YbB}_{12}$  and  $\text{Yb}_{0.99}\text{Lu}_{0.01}\text{B}_{12}$  provide evidence for another interpretation of the low temperature relaxation enhancement, namely that it may be driven by fluctuations of defect-induced magnetic centers and spin-diffusion-assisted relaxation [45]. These  $\text{YbB}_{12}$  results motivate further measurements and comparison of  $^{11}\text{B}$  and  $^{10}\text{B}$   $T_1^{-1}$  in  $\text{PuB}_4$ .

To conclude, we have performed  $^{239}\text{Pu}$  NMR measurements for the second time ever in powdered and single crystalline  $\text{PuB}_4$ . We extracted the isotropic and anisotropic shifts from the uniaxially symmetric powder pattern and demonstrate that one can observe the  $^{239}\text{Pu}$  NMR signal in anisotropic environments and up to room temperature. The large contrast of the orbital shift between the purely ionic insulator  $\text{PuO}_2$  ( $\sim +24.7\%$ ) and band insulator  $\text{PuB}_4$  ( $\sim -0.5\%$ ) provide us with new tool to investigate the nature of the chemical bond based on the value of the  $^{239}\text{Pu}$  shift. Single crystal  $^{239}\text{Pu}$  NMR measurements of  $K_c(T)$  and  $T_1^{-1}(T)$  provide unique access to bulk gap-like behavior with an energy gap that is only slightly suppressed with respect to DFT+SOC calculations, and  $T_1^{-1}(T)$  also evidences the existence of bulk in-gap states. Our confirmation of a bulk gap motivate future surface sensitive measurements to confirm the theoretical prediction that  $\text{PuB}_4$  is a topological insulator.

#### ACKNOWLEDGMENTS

The authors would like to thank D. L. Clark, Z. Fisk, P. F. S. Rosa, A. M. Mounce, S. Seo, R. Movshovich, M. Janoschek, D.-Y. Kim, D. Fobes, N. Sung, N. Leon-Brito,

M. W. Malone, H.-J. Grafe, M. Požek, D. Kasinathan and P. Coleman for stimulating discussions. Work at Los Alamos National Laboratory was performed with the support of the Los Alamos LDRD program. TEA-S was supported as part of the Center for Actinide Science and Technology (CAST), an Energy Frontier Research Center funded by the U.S. Department of Energy, Office of Science, Basic Energy Sciences under Award Number DE-SC0016568. HS was also partly supported by JSPS KAKENHI Grant Number JP16KK0106. APD acknowledges a Director's Postdoctoral Fellowship supported through the Los Alamos LDRD program.

---

\* [adioguardi@gmail.com](mailto:adioguardi@gmail.com)

- [1] M. Z. Hasan and C. L. Kane, "Colloquium: Topological insulators," *Rev. Mod. Phys.* **82**, 3045–3067 (2010).
- [2] Xiao-Liang Qi and Shou-Cheng Zhang, "Topological insulators and superconductors," *Rev. Mod. Phys.* **83**, 1057–1110 (2011).
- [3] P. Coleman, "Heavy Fermions: electrons at the edge of magnetism," in *Handbook of Magnetism and Advanced Magnetic Materials: Fundamentals and Theory*, edited by H. Kronmüller and S. Parkin (J. Wiley and Sons, 2007) pp. 95–148.
- [4] Maxim Dzero, Kai Sun, Victor Galitski, and Piers Coleman, "Topological kondo insulators," *Phys. Rev. Lett.* **104**, 106408 (2010).
- [5] Maxim Dzero, Jing Xia, Victor Galitski, and Piers Coleman, "Topological kondo insulators," *Annual Review of Condensed Matter Physics* **7**, 249–280 (2015).
- [6] Tetsuya Takimoto, "SmB<sub>6</sub>: A promising candidate for a topological insulator," *Journal of the Physical Society of Japan* **80**, 123710 (2011).
- [7] D. J. Kim, S. Thomas, T. Grant, J. Botimer, Z. Fisk, and Jing Xia, "Surface hall effect and nonlocal transport in SmB<sub>6</sub>: Evidence for surface conduction," *Scientific Reports* **3**, 3150 (2013).
- [8] M. Neupane, N. Alidoust, S.-Y. Xu, T. Kondo, Y. Ishida, D. J. Kim, Chang Liu, I. Belopolski, Y. J. Jo, T.-R. Chang, H.-T. Jeng, T. Durakiewicz, L. Balicas, H. Lin, A. Bansil, S. Shin, Z. Fisk, and M. Z. Hasan, "Surface electronic structure of the topological kondo-insulator candidate correlated electron system SmB<sub>6</sub>," *Nature Communications* **4**, 2991 (2013).
- [9] J. Jiang, S. Li, T. Zhang, Z. Sun, F. Chen, Z.R. Ye, M. Xu, Q.Q. Ge, S.Y. Tan, X.H. Niu, M. Xia, B.P. Xie, Y.F. Li, X.H. Chen, H.H. Wen, and D.L. Feng, "Observation of possible topological in-gap surface states in the kondo insulator SmB<sub>6</sub> by photoemission," *Nature Communications* **4**, 3010 (2013).
- [10] Kevin T. Moore and Gerrit van der Laan, "Nature of the 5f states in actinide metals," *Rev. Mod. Phys.* **81**, 235–298 (2009).
- [11] David L. Clark, "The chemical complexities of plutonium," *Los Alamos Science* **26**, 364–381 (2000).
- [12] Xiaoyu Deng, Kristjan Haule, and Gabriel Kotliar, "Plutonium Hexaboride is a Correlated Topological Insulator," *Phys. Rev. Lett.* **111**, 176404 (2013).
- [13] J. H. Shim, K. Haule, and G. Kotliar, "Fluctuating va-

- lence in a correlated solid and the anomalous properties of  $\delta$ -plutonium,” *Nature* **446**, 513–516 (2007).
- [14] M. Janoschek, P. Das, B. Chakrabarti, D. L. Abernathy, M. D. Lumsden, J. M. Lawrence, J. D. Thompson, G. H. Lander, J. N. Mitchell, S. Richmond, M. Ramos, F. Trouw, J.-X. Zhu, K. Haule, G. Kotliar, and E. D. Bauer, “The valence-fluctuating ground state of plutonium,” *Science Advances* **1**, e1500188 (2015).
- [15] David L. Clark, Siegfried S. Hecker, Gordon D. Jarvinen, and Mary P. Neu, “Plutonium,” in *The Chemistry of the Actinide and Transactinide Elements* (Springer Netherlands, Dordrecht, 2006) pp. 813–1264.
- [16] J. C. Lashley, A. Lawson, R. J. McQueeney, and G. H. Lander, “Absence of magnetic moments in plutonium,” *Phys. Rev. B* **72**, 054416 (2005).
- [17] E D Bauer and J D Thompson, “Plutonium-Based Heavy-Fermion Systems,” *Annual Review of Condensed Matter Physics* **6**, 137–153 (2015).
- [18] Xiao Zhang, Haijun Zhang, Jing Wang, Claudia Felser, and Shou-Cheng Zhang, “Actinide topological insulator materials with strong interaction,” *Science* **335**, 1464–1466 (2012).
- [19] Hongchul Choi, Wei Zhu, S. K. Cary, L. E. Winter, Zhoushen Huang, R. D. McDonald, V. Mocko, B. L. Scott, P. H. Tobash, J. D. Thompson, S. A. Kozimor, E. D. Bauer, Jian-Xin Zhu, and F. Ronning, “Experimental and theoretical study of topology and electronic correlations in  $\text{PuB}_4$ ,” *Phys. Rev. B* **97**, 201114 (2018).
- [20] J. C. Cooley, M. C. Aronson, Z. Fisk, and P. C. Canfield, “ $\text{SmB}_6$ : Kondo insulator or exotic metal?” *Phys. Rev. Lett.* **74**, 1629–1632 (1995).
- [21] B. J. McDonald and W. I. Stuart, “The crystal structure of some plutonium borides,” *Acta Crystallographica* **13**, 447–448 (1960).
- [22] Harry A Eick, “Plutonium Borides,” *Inorganic Chemistry* **4**, 1237–1239 (1965).
- [23] P Rogl and P E Potter, “The B-Pu (boron-plutonium) system,” *Journal of Phase Equilibria* **18**, 467–473 (1997).
- [24] J. L. Smith and H. H. Hill, “Magnetism in neptunium borides,” in *AIP Conference Proceedings Vol. 24* (American Institute of Physics, 1975) pp. 382–383.
- [25] Koichi Momma and Fujio Izumi, “VESTA 3 for three-dimensional visualization of crystal, volumetric and morphology data,” *Journal of Applied Crystallography* **44**, 1272–1276 (2011).
- [26] H. Yasuoka, G. Koutroulakis, H. Chudo, S. Richmond, D. K. Veirs, A. I. Smith, E. D. Bauer, J. D. Thompson, G. D. Jarvinen, and D. L. Clark, “Observation of  $^{239}\text{Pu}$  Nuclear Magnetic Resonance,” *Science* **336**, 901–904 (2012).
- [27] C. P. Slichter, *Principles of magnetic resonance*, Springer series in solid-state sciences (Springer-Verlag, 1990).
- [28] Nicholas J Curro, “Nuclear magnetic resonance in Kondo lattice systems,” *Reports on Progress in Physics* **79**, 064501 (2016).
- [29] A. W. Kinross, M. Fu, T. J. Munsie, H. A. Dabkowska, G. M. Luke, Subir Sachdev, and T. Imai, “Evolution of Quantum Fluctuations Near the Quantum Critical Point of the Transverse Field Ising Chain System  $\text{CoNb}_2\text{O}_6$ ,” *Phys. Rev. X* **4**, 031008 (2014).
- [30] Sharon E. Ashbrook, John M. Griffin, and Karen E. Johnston, “Recent Advances in Solid-State Nuclear Magnetic Resonance Spectroscopy,” *Annual Review of Analytical Chemistry* **11**, 1–24 (2018).
- [31] J Butterworth, “The nuclear magnetic moment of plutonium-239,” *Philosophical Magazine* **3**, 1053–1054 (1958).
- [32] K. Ikushima, S. Tsutsui, Y. Haga, H. Yasuoka, R. E. Walstedt, N. M. Masaki, A. Nakamura, S. Nasu, and Y. Ōnuki, “First-order phase transition in  $\text{UO}_2$ :  $^{235}\text{U}$  and  $^{17}\text{O}$  NMR study,” *Phys. Rev. B* **63**, 104404 (2001).
- [33] K. Ikushima, Y. Kato, M. Takigawa, F. Iga, S. Hiura, and T. Takabatake, “ $^{171}\text{Yb}$  NMR in the Kondo semiconductor  $\text{YbB}_{12}$ ,” *Physica B: Condensed Matter* **281-282**, 274–275 (2000).
- [34] See Supplemental Material at [URL will be inserted by publisher] for further information including experimental and theoretical methods, control experiment,  $^{239}\text{Pu}$  hyperfine coupling analysis,  $^{239}\text{Pu}$  gap fitting procedure,  $^{239}\text{Pu}$  spin-lattice relaxation rate anisotropy, and  $^{11}\text{B}$  powder NMR results. The Supplemental Material includes references [24, 26, 37, 38, 40, 46–54].
- [35] Chuck-Hou Yee, Gabriel Kotliar, and Kristjan Haule, “Valence fluctuations and quasiparticle multiplets in plutonium chalcogenides and pnictides,” *Physical Review B* **81**, 035105 (2010).
- [36] Jian-Xin Zhu, R. C. Albers, K. Haule, G. Kotliar, and J. M. Wills, “Site-selective electronic correlation in  $\alpha$ -plutonium metal,” *Nature Communications* **4**, 2644 (2013).
- [37] D. C. Johnston, “Stretched exponential relaxation arising from a continuous sum of exponential decays,” *Phys. Rev. B* **74**, 184430 (2006).
- [38] C. H. Booth, Yu Jiang, S. A. Medling, D. L. Wang, A. L. Costello, D. S. Schwartz, J. N. Mitchell, P. H. Tobash, E. D. Bauer, S. K. McCall, M. A. Wall, and P. G. Allen, “Self-irradiation damage to the local structure of plutonium and plutonium intermetallics,” *J Appl Phys* **113**, 093502 (2013).
- [39] Masashi Takigawa, Hiroshi Yasuoka, Yoshio Kitaoka, Takaho Tanaka, Hiroshi Nozaki, and Yoshio Ishizawa, “NMR Study of a Valence Fluctuating Compound  $\text{SmB}_6$ ,” *Journal of the Physical Society of Japan* **50**, 2525–2532 (1981).
- [40] T. Caldwell, A. P. Reyes, W. G. Moulton, P. L. Kuhns, M. J. R. Hoch, P. Schlottmann, and Z. Fisk, “High-field suppression of in-gap states in the Kondo insulator  $\text{SmB}_6$ ,” *Phys. Rev. B* **75**, 075106 (2007).
- [41] A. P. Reyes, R. H. Heffner, P. C. Canfield, J. D. Thompson, and Z. Fisk, “ $^{209}\text{Bi}$  NMR and NQR investigation of the small-gap semiconductor  $\text{Ce}_3\text{Bi}_4\text{Pt}_3$ ,” *Phys. Rev. B* **49**, 16321–16330 (1994).
- [42] Yutaka Itoh and Hiroshi Yasuoka, “Interrelation between Dynamical and Static Spin Gaps in Quantum Spin Systems,” *Journal of the Physical Society of Japan* **66**, 334–336 (1997).
- [43] Dimitrios Koumoulis, Thomas C. Chasapis, Robert E. Taylor, Michael P. Lake, Danny King, Nanette N. Jarenwattananon, Gregory A. Fiete, Mercouri G. Kanatzidis, and Louis-S. Bouchard, “NMR Probe of Metallic States in Nanoscale Topological Insulators,” *Phys. Rev. Lett.* **110**, 026602 (2013).
- [44] Tetsuya Takimoto, “ $\text{SmB}_6$ : A promising candidate for a topological insulator,” *Journal of the Physical Society of Japan* **80**, 123710 (2011).
- [45] Naohito Shishiuchi, Yoshitomo Kato, Oleg M Vyaselev, Masashi Takigawa, Sayaka Hiura, Fumitoshi Iga, and Toshiro Takabatake, “Defect-induced magnetic fluctua-

- tions in YbB12,” *Journal of Physics and Chemistry of Solids* **63**, 1231–1234 (2002).
- [46] Karlheinz Schwarz and Peter Blaha, “Solid state calculations using WIEN2k,” *Computational Materials Science* **28**, 259–273 (2003).
- [47] John P. Perdew, Kieron Burke, and Matthias Ernzerhof, “Generalized Gradient Approximation Made Simple,” *Phys. Rev. Lett.* **77**, 3865–3868 (1996).
- [48] P. Blaha, K. Schwarz, and P. Herzig, “First-Principles Calculation of the Electric Field Gradient of Li<sub>3</sub>N,” *Phys. Rev. Lett.* **54**, 1192–1195 (1985).
- [49] G. Kotliar, S. Y. Savrasov, K. Haule, V. S. Oudovenko, O. Parcollet, and C. A. Marianetti, “Electronic structure calculations with dynamical mean-field theory,” *Rev. Mod. Phys.* **78**, 865–951 (2006).
- [50] Kristjan Haule, Chuck-Hou Yee, and Kyoo Kim, “Dynamical mean-field theory within the full-potential methods: Electronic structure of CeIrIn<sub>5</sub>, CeCoIn<sub>5</sub>, and CeRhIn<sub>5</sub>,” *Phys. Rev. B* **81**, 195107 (2010).
- [51] Philipp Werner and Andrew J. Millis, “Hybridization expansion impurity solver: General formulation and application to Kondo lattice and two-orbital models,” *Phys. Rev. B* **74**, 155107 (2006).
- [52] Kristjan Haule, “Quantum monte carlo impurity solver for cluster dynamical mean-field theory and electronic structure calculations with adjustable cluster base,” *Phys. Rev. B* **75**, 155113 (2007).
- [53] DM Nisson and NJ Curro, “Nuclear magnetic resonance Knight shifts in the presence of strong spinorbit and crystal-field potentials,” *New Journal of Physics* **18**, 073041 (2016).
- [54] Robin K. Harris, Edwin D. Becker, Sonia M. Cabral De Menezes, Robin Goodfellow, and Pierre Granger, “NMR nomenclature. Nuclear spin properties and conventions for chemical shifts (IUPAC Recommendations 2001),” *Pure and Applied Chemistry* **73**, 1795–1818 (2001).